



# HHS Public Access

Author manuscript

*Cell Host Microbe*. Author manuscript; available in PMC 2018 November 08.

Published in final edited form as:

*Cell Host Microbe*. 2017 November 08; 22(5): 667–677.e5. doi:10.1016/j.chom.2017.10.008.

## ***Staphylococcus aureus* virulent PSM $\alpha$ peptides induce keratinocyte alarmin release to orchestrate IL-17-dependent skin inflammation**

Seitaro Nakagawa<sup>1,5</sup>, Masanori Matsumoto<sup>2,5</sup>, Yuki Katayama<sup>1</sup>, Rena Oguma<sup>1</sup>, Seiichiro Wakabayashi<sup>1</sup>, Tyler Nygaard<sup>2</sup>, Shinobu Saijo<sup>3</sup>, Naohiro Inohara<sup>2</sup>, Michael Otto<sup>4</sup>, Hiroyuki Matsue<sup>1,3</sup>, Gabriel Núñez<sup>2,6,\*</sup>, and Yuumi Nakamura<sup>1,\*</sup>

<sup>1</sup>Department of Dermatology, Chiba University Graduate School of Medicine, Chiba, 260-8670, Japan

<sup>2</sup>Department of Pathology and Comprehensive Cancer Center, The University of Michigan Medical School, Ann Arbor, MI 48109, USA

<sup>3</sup>Division of Molecular Immunology, Medical Mycology Research Center, Chiba University, Chiba, 260-8673, Japan

<sup>4</sup>Pathogen Molecular Genetics Section, Laboratory of Human Bacterial Pathogenesis, National Institute of Allergy and Infectious Diseases, National Institutes of Health, Bethesda, MD 20892, USA

### **Summary**

*Staphylococcus aureus* commonly colonizes the epidermis, but the mechanisms by which the host senses virulent but not commensal *S. aureus* to trigger inflammation remain unclear. Using a murine epicutaneous infection model, we found that *S. aureus* expressed phenol-soluble modulin (PSM) $\alpha$ , a group of secreted virulence peptides, is required to trigger cutaneous inflammation. PSM $\alpha$  induces the release of keratinocyte IL-1 $\alpha$  and IL-36 $\alpha$ , and signaling via IL-1R and IL-36R was required for induction of the pro-inflammatory cytokine IL-17. The levels of released IL-1 $\alpha$  and IL-36 $\alpha$ , as well as IL-17 production by  $\gamma\delta$  T cells and ILC3 and neutrophil infiltration to the site of infection were greatly reduced in mice with total or keratinocyte-specific deletion of the IL-1R and IL-36R signaling adaptor Myd88. Further, *Il17a*<sup>-/-</sup>*f*<sup>-/-</sup> mice showed blunted *S. aureus*-

\*Correspondence: gabriel.nunez@umich.edu (G.N.) and yumi01@chiba-u.jp (Y.N.).

<sup>5</sup>These authors contributed equally

<sup>6</sup>Lead author

#### **Author Contributions**

Designed experiments, S.N., M.M., G.N. and Y.N.; Performed experiments, S.N., M.M., Y.K., R.O., S.W., T.N., S.S. and Y.N.; Provided critical reagents and scientific insight, M. O.; Analyzed data, S.N., M.M., N.I., H.M., G.N. and Y.N.; S. N., M. M., G.N. and Y.N. wrote the paper.

#### **Competing Financial Interests**

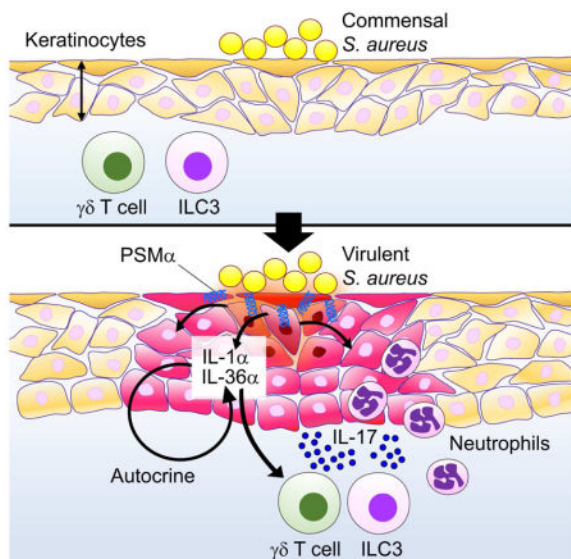
The authors declare no competing financial interests.

**Publisher's Disclaimer:** This is a PDF file of an unedited manuscript that has been accepted for publication. As a service to our customers we are providing this early version of the manuscript. The manuscript will undergo copyediting, typesetting, and review of the resulting proof before it is published in its final citable form. Please note that during the production process errors may be discovered which could affect the content, and all legal disclaimers that apply to the journal pertain.

induced inflammation. Thus, keratinocyte Myd88 signaling in response to *S. aureus* PSM $\alpha$  drives an IL-17-mediated skin inflammatory response to epicutaneous *S. aureus* infection.

### In Brief (eTOC Blurp)

Nakagawa *et al.* demonstrate that *S. aureus* produces PSM $\alpha$ , a group of virulence peptides, to induce keratinocyte damage and release of IL-1 $\alpha$  and IL-36 $\alpha$ . IL-1R and IL-36R signaling via the adaptor Myd88 induces IL-17-producing  $\gamma\delta$  T cells and ILC3, which critically mediate skin inflammation in response to epicutaneous *S. aureus*.



### Keywords

alarmins; IL-1; IL-36; Myd88; *S. aureus*; skin infection; pathogen virulence

### Introduction

The skin is the largest organ at the interface between the external environment and host tissues. The epidermis located on the skin surface is important in maintaining the physical and immunological barrier of the skin by protecting the host from harmful environmental stimuli including invasive microbes (Segre, 2006). *Staphylococcus aureus*, a Gram-positive bacterium, is a leading cause of human infection capable of invading most tissues of the human body. The superficial skin is a major infection site for *S. aureus*, which normally resides in 10–20% of healthy individuals (Lowy, 1998). The *S. aureus* causing skin infections often originate from resident bacteria that colonize the mucosal surfaces of the skin (Balasubramanian et al., 2017; Lowy, 1998). How *S. aureus* produces virulence factors to transform from a skin commensal to a pathogen is poorly understood. Previous studies suggested that this might be a consequence of activation of virulence gene regulatory networks in response to environmental signals (Novick and Geisinger, 2008). A major *S. aureus* virulence program is the accessory gene regulatory (Agr) quorum-sensing, a two-component system that responds to bacterial density (Novick, 2003). Upon activation, the

*agr* locus induces the expression of a wide array of secreted virulence factors including toxins and enzymes that are important for the adaptation of the pathogen to the environment (Novick, 2003). Agr-regulated toxins include phenol-soluble modulins (PSMs), a group of seven different peptides divided into  $\alpha$ - and  $\beta$ -type PSMs (Cheung et al., 2014). PSM peptides form amphipathic  $\alpha$ -helical structures capable of forming pores in artificial membranes (Wang et al., 2007). PSM $\alpha$  peptides are highly cytotoxic to a wide variety of cells including keratinocytes (KCs) while other PSMs have very limited cytotoxic activities (Nakamura et al., 2013; Wang et al., 2007). In a mouse epicutaneous model of *S. aureus* infection,  $\delta$ -toxin, a PSM peptide, promotes skin inflammation by inducing mast cell degranulation (Nakamura et al., 2013). However, the mechanism by which *S. aureus* interacts with KCs to trigger skin inflammation *in vivo* remains largely unknown.

KCs are the predominant cell type in the stratified epithelial layer of the epidermis. In response to environmental stimuli, KCs produce a wide variety of molecules including multiple cytokines, chemokines and anti-microbial peptides (Kennedy-Crispin et al., 2012; Nestle et al., 2009). Some of these KC molecules, including IL-1 $\alpha$ , high-mobility group box 1 (HMGB1) protein and anti-microbial peptides, can be released upon tissue damage and function as 'alarmins' to activate the immune system (Rider et al., 2017; Yang et al., 2009). However, the role of KCs in *S. aureus*-induced inflammation *in vivo* is poorly understood because practically all cutaneous models of *S. aureus* infection rely on subepidermal inoculation or prior physical disruption of the epidermis (Miller et al., 2006; Wang et al., 2007). In the intradermal or subcutaneous model of *S. aureus* infection, mice deficient in Myd88, the adaptor molecule that is critical for signaling through the Toll-like receptor (TLR)/IL-1/IL-18 family of receptors, showed increased inflammation, abscess formation and epidermal ulceration which correlated with impaired *S. aureus* clearance (Miller et al., 2006). Furthermore, *Il1r*<sup>-/-</sup>, but not *Tlr2*<sup>-/-</sup>, mice showed increased inflammation and abscess formation in the subcutaneous infection model (Miller et al., 2006). However, the role of these signaling pathways in promoting inflammation after epidermal colonization of *S. aureus* remains unclear. Using conditions in which virulence genes are induced upon epidermal colonization, we show that *S. aureus* relies on virulent Agr-regulated PSM $\alpha$  peptides to trigger cutaneous inflammation. PSM $\alpha$  induces the release of IL-1 $\alpha$  and IL-36 from KCs to orchestrate cutaneous inflammation via Myd88 signaling and IL-17 production.

## Results

### Keratinocyte Myd88 is essential for *S. aureus*-induced skin inflammation

We used a recently developed model of *S. aureus* colonization that induces Agr-regulated virulence to investigate the mechanism by which the pathogen triggers cutaneous inflammation (Nakamura et al., 2013). In this epicutaneous model, wild-type (WT) mice infected with *S. aureus* (strain LAC, pulsed-field type USA300) showed severe skin disease and inflammation characterized by neutrophil infiltrates and epidermal thickening on day 7 after colonization (Figures 1A, 1B, 1D and 1E). In contrast, *Myd88*<sup>-/-</sup> mice showed little skin pathology when compared with WT mice (Figures 1A–1E). Unlike the epicutaneous model, *Myd88*<sup>-/-</sup> mice infected intradermally with *S. aureus* showed increased skin pathology and pathogen loads compared to that observed in WT-infected mice (Figures

S1A–S1C), which is consistent with a previous report (Miller et al., 2006). In contrast, *Myd88*<sup>-/-</sup> mice exhibited lower *S. aureus* CFUs than WT mice in the epicutaneous model (Figure 1C), suggesting that Myd88-dependent inflammation promotes pathogen colonization in this model. Thus, the route of infection is critical to revealing the function of innate signaling pathways in host defense against *S. aureus* in the skin. To determine whether Myd88 acts within KCs, we crossed mice with a floxed exon of Myd88 (*Myd88*<sup>fl/fl</sup> mice) with a keratin 14 (K14)-Cre mouse deleter strain to generate *K14-Cre-Myd88*<sup>fl/fl</sup> mice with conditional deletion of Myd88 within KCs. Notably, mice lacking Myd88 in KCs (*Myd88*<sup>ker</sup>) showed a phenotype similar to that observed in mice with whole-body deletion of Myd88 (Figures 1A, 1B and 1D). However, pathogen loads were comparable in *Myd88*<sup>ker</sup> mice and WT mice (Figure 1C). Furthermore, the reduction in epidermal thickening in *Myd88*<sup>ker</sup> mice was not as prominent as in *Myd88*<sup>-/-</sup> mice (Figure 1E). In contrast to the epicutaneous model, *Myd88*<sup>ker</sup> and WT mice showed comparable skin inflammation in response to intradermal *S. aureus* infection (Figures S1D–S1F). These results indicate a critical role for Myd88 and particularly Myd88 in KCs for the induction of immune responses to *S. aureus* in the epicutaneous infection model.

### **IL-1R and IL-36R are essential for induction of skin inflammation in epicutaneous *S. aureus* infection**

Myd88 is a critical adaptor molecule required for signaling via multiple immune receptors, including TLR/IL-1R/IL-18R/IL-36R (Palomo et al., 2015; Takeuchi and Akira, 2002). Initial experiments showed that deficiency in TLR2, TLR4 or IL-18 did not affect either skin disease, histopathology or pathogen loads in the epicutaneous model of *S. aureus* infection (Figures S2A and S2B). In contrast, mice deficient in IL-1R, which can be stimulated by either IL-1 $\alpha$  or IL-1 $\beta$ , exhibited a reduction in disease score, neutrophil infiltrates and epidermal thickening, despite similar pathogen loads when compared with WT mice (Figures 2A–2E). Two related cytokines IL-36 $\alpha$  and IL-36 $\gamma$  are expressed in KCs (Gresnigt and van de Veerdonk, 2013) and activate the IL-36R that also signals via Myd88 (Towne et al., 2004). Administration of a neutralizing monoclonal antibody (Mab) against IL-36R also reduced neutrophil infiltration and epidermal thickening induced by epicutaneous *S. aureus* infection without affecting pathogen loads (Figures 2C–2E). Treatment of *Il1r*<sup>-/-</sup> mice with the neutralizing anti-IL-36R Mab further reduced the disease score, neutrophil infiltration and epidermal thickening when compared WT mice (Figures 2A, 2B, 2D and 2E). These results indicate that both IL-1R and IL-36R signaling contribute to skin inflammation induced by *S. aureus* infection.

### ***S. aureus* induces IL-1 $\alpha$ and IL-36 $\alpha$ expression via Myd88 in keratinocytes**

Given that IL-1R signaling is important for *S. aureus*-induced inflammation, we asked whether IL-1 $\alpha$  or IL-1 $\beta$  mediates skin pathology in the epicutaneous infection model. Infection with *S. aureus* showed comparable pathology, disease scores and pathogen loads in WT and *Il1 $\beta$* <sup>-/-</sup> mice (Figure S2C). In contrast, neutralization of IL-1 $\alpha$  with a Mab reduced skin pathology without affecting pathogen loads, compared with mice treated with isotype-matched control Mab (Figures 3A–3C). Epicutaneous infection of *S. aureus* in WT mice substantially enhanced the expression of IL-1 $\alpha$  and IL-36 $\alpha$  in the upper area of the epidermis, which was reduced in *Myd88*<sup>ker</sup> and *Myd88*<sup>-/-</sup> mice (Figures 3D and S3).

Consistent with results showed in Figure 1C, pathogen loads were reduced in the skin of *Myd88*<sup>-/-</sup> mice compared to WT and *Myd88*<sup>ker</sup> (Figure 3E). To determine whether *S. aureus* produces molecules that induce IL-1 $\alpha$  and IL-36 $\alpha$  release from KCs, primary KCs from WT and *Myd88*<sup>-/-</sup> mice were cultured under conditions that promote their terminal differentiation (Bikle et al., 2012) and then incubated with supernatants of *S. aureus* cultures. There was marked release of IL-1 $\alpha$  and IL-36 $\alpha$  after 60 min incubation of WT KCs with *S. aureus* culture supernatants (Figures 3F and 3G). Notably, the release of IL-1 $\alpha$  and IL-36 $\alpha$  was reduced in KCs from *Myd88*<sup>-/-</sup> mice (Figures 3F and 3G). Furthermore, the KC release of IL-1 $\alpha$  was markedly reduced and that of IL-36 $\alpha$  was partially affected in KC deficient in IL-1R (Figures 3H and 3I), suggesting that IL-1 $\alpha$  release enhances IL-1 $\alpha$  and IL-36 $\alpha$  production via IL-1R signaling in KCs. In addition, IL-36 $\alpha$  release by *S. aureus* was inhibited by neutralization of IL-36R whereas that of IL-1 $\alpha$  was only minimally affected (Figures 3J and 3K). Collectively these results indicate that IL-1 $\alpha$  and IL36 $\alpha$  production are regulated by *S. aureus* stimulation via Myd88 signaling in KCs.

### IL-17 is critical for *S. aureus*-induced skin inflammation

Members of the IL-1 family of cytokines are important for the induction of cellular immune responses and production of several cytokines including IL-17 and IL-22 (Sonnenberg et al., 2011; Villarino and Laurence, 2015). To determine which cytokines are induced upon epicutaneous infection with *S. aureus*, we assessed the production of multiple cytokines by skin immune cells at the peak of inflammation. Total skin cells were gated on hematopoietic CD45<sup>+</sup>CD90<sup>+</sup> cells and the number of CD45<sup>+</sup>CD90<sup>+</sup> cells producing IL-17A, IL-17F, IL-22, interferon- $\gamma$  (IFN- $\gamma$ ) and GM-CSF was measured by flow cytometry. The analysis revealed that epicutaneous *S. aureus* infection induces a marked increase in the number of IL-17A-producing cells and a modest increase in cells producing IL-17F and IL-22 while there was minimal or no induction of IFN- $\gamma$  and GM-CSF-producing cells (Figure 4A). The number of leukocytes infiltrating the skin including IL-17A-producing cells, was reduced in *Myd88*<sup>-/-</sup> mice (Figure 4B). Furthermore, the production of IL17A was reduced in the skin of *Myd88*<sup>ker</sup> and *Il1r*<sup>-/-</sup> mice injected with IL-36R neutralizing Mab (Figure 4C). The production of IL-17F was also reduced in *Il1r*<sup>-/-</sup> mice injected with IL-36R neutralizing Mab compared to WT mice (Figure 4C). To determine if IL-17 was important for the induction of skin inflammation, WT mice and mice doubly deficient in IL-17A and IL-17F were infected epicutaneously with *S. aureus*. We found that *Il17a*<sup>-/-f</sup> mice exhibited greatly reduced skin disease scores and neutrophil infiltration, but normal pathogen loads, compared with WT mice (Figures 4D–4H). In contrast, WT and *Il22*<sup>-/-</sup> mice showed comparable skin phenotype after *S. aureus* infection (Figure S2D). These results indicate that *S. aureus* induces IL-17 via Myd88 signaling which is critical for inflammatory pathology in the skin.

### $\gamma\delta$ T cells and type 3 innate lymphoid cells are the main producers of IL-17 in response to skin infection

We next asked which immune cell population(s) produces IL-17 in response to epicutaneous *S. aureus* infection. Gating on CD45<sup>+</sup> cells revealed two populations of IL-17<sup>+</sup>CD90<sup>+</sup> cells in the skin of mice epicutaneously infected with *S. aureus* (Figure 5A). These included  $\gamma\delta$ <sup>intermediate</sup> dermal  $\gamma\delta$  T cells and lineage-negative CD45<sup>+</sup>CD90<sup>+</sup> immune cells which



marks type 3 innate lymphoid cells (ILC3) (Figure 5A). To determine whether  $\gamma\delta$  T cells contribute to skin inflammation in response to *S. aureus*, we infected WT and *Tcr $\delta$ <sup>-/-</sup>* mice with the pathogen and assessed the pathology and disease scores in the skin. We found comparable disease scores, but reduced neutrophil infiltration in *Tcr $\delta$ <sup>-/-</sup>* mice compared with WT mice (Figures 5B–5F). As expected, IL-17-producing  $\gamma\delta$  T cells were absent in the skin of infected *Tcr $\delta$ <sup>-/-</sup>* mice, but the population of IL-17-producing ILC was unchanged in *Tcr $\delta$ <sup>-/-</sup>* mice (Figure 5G). To determine whether ILC3 contribute to skin inflammation, we treated *Tcr $\delta$ <sup>-/-</sup>* mice with anti-CD90 Mab to deplete the ILC3 population (Figure S4) and infected the treated mice epicutaneously with *S. aureus*. Treatment with anti-CD90 Mab significantly reduced skin disease scores without affecting pathogen loads in *Tcr $\delta$ <sup>-/-</sup>* mice when compared with mutant mice treated with control Mab (Figures 5H–5J). These results indicate that both ILC3 and  $\gamma\delta$  T cells contribute to skin inflammation in response to epicutaneous *S. aureus* infection.

### ***S. aureus* PSM $\alpha$ induces keratinocyte IL-1 $\alpha$ and IL-36 $\alpha$ release to mediate skin inflammation**

We next assessed which factor(s) released by *S. aureus* is important for eliciting the release of IL-1 $\alpha$  and IL-36 $\alpha$  from KCs and thereby triggering IL-17-dependent skin inflammation. PSMs including the peptides PSM $\alpha$ 1 through PSM $\alpha$ 4 induce robust cell death of mouse KCs *in vitro* (Nakamura et al., 2013). Because the Agr virulence system that controls the production of PSM $\alpha$  is activated during epicutaneous *S. aureus* infection in our model (Nakamura et al., 2013), we asked whether PSM $\alpha$  is important for eliciting skin inflammation. We first assessed whether PSM $\alpha$  is important for the release of IL-1 $\alpha$  and IL-36 $\alpha$  by incubating primary mouse KCs with culture supernatants from WT or isogenic *S. aureus* mutant strains deficient in PSM $\alpha$ 1–4 (*psma*) or PSM $\beta$ 1–2 (*psm $\beta$* ). Incubation with the culture supernatant from WT and mutant *psm $\beta$* , but not mutant *psma*, strain induced cell death and release of IL-1 $\alpha$  and IL-36 $\alpha$  (Figures 6A–6C, S5A–S5B). In addition to mouse KCs, human KCs showed a marked release of IL-1 $\alpha$  and enhanced cytotoxicity after treatment with supernatants from the WT and mutant *psm $\beta$*  strains, but not mutant *psma* (Figures S6A–S6B). Complementation of mutant *psma* *S. aureus* with *psma* plasmid restored cytotoxicity and cytokine release in both mouse and human KCs (Figures S5F–S5G, S6C–S6D). In addition, stimulation of human KCs with synthetic PSM $\alpha$ 3 peptide induced IL-1 $\alpha$  release and cytotoxicity (Figures S6E–S6F). Furthermore, pre-treatment with anakinra, an IL-1R antagonist, reduced IL-1 $\alpha$  release induced by PSM $\alpha$ 3 peptide without affecting cytotoxicity (Figures S6G–S6H). To determine whether PSM $\alpha$  is important for the induction of skin inflammation, we infected WT mice with WT and mutant *psma* and *psm $\beta$*  *S. aureus* strains using the epicutaneous model. Histological analysis revealed that the ability of the *psma* mutant strain to induce skin disease, epidermal thickening and neutrophil infiltration were impaired compared with the WT and *psm $\beta$*  strains (Figures 6D, 6E, 6G, 6H, S5C and S5D). There were reduced pathogen loads and IL-17 production in the skin of mice infected with the *psma* mutant strain when compared to the WT bacterium (Figures 6F, 6I, and S5E). These results suggest that PSM $\alpha$  from *S. aureus* is a key virulence factor for triggering *S. aureus*-induced skin inflammation.

## Discussion

The mechanism by which *S. aureus* triggers skin inflammation in response to epidermal colonization has remained largely unknown. The paucity of knowledge is largely explained by the lack of a model of epidermal infection that mimics the virulent lifestyle of the pathogen. Using conditions in which *S. aureus* colonizes the epidermis and induces virulence (Nakamura et al., 2013), we found that Agr-regulated PSM $\alpha$  peptides trigger the release of the KC alarmins IL-1 $\alpha$  and IL-36 $\alpha$  to elicit skin inflammation. These observations indicate that the host senses the pathogen indirectly through the induction of KC damage triggered by cytotoxic virulence factors. Because expression of aggressive, cytolytic PSMs appears to be limited mostly to *S. aureus* in comparison to *S. epidermidis* (Cheung et al., 2010), these observations suggest a model in which the host immune system can discriminate a virulent pathogen from commensals by sensing KC damage. Because PSM $\alpha$  peptides have been shown to induce chemokines from neutrophils (Kretschmer et al., 2010; Wang et al., 2007), it is possible that PSM $\alpha$  also contribute to skin inflammation via KC-independent mechanisms. Previous work showed that epidermal colonization of some commensals can induce IL-17-producing CD8<sup>+</sup> cells in the dermis (Naik et al., 2015; Naik et al., 2012). However, colonization by commensals does not trigger overt inflammation and skin pathology including epidermal thickening and neutrophil recruitment which is observed after *S. aureus* infection (Naik et al., 2015). This model also implies that the host senses not the bacterium *per se*, but the virulent state of the pathogen through PSM $\alpha$ -induced release of KC alarmins. *S. aureus* lacking PSM $\alpha$  peptides accumulate at lower numbers than the WT bacterium after epicutaneous colonization. These results suggest that the pathogen benefits from PSM $\alpha$  production, at least in part, by inducing the release of nutrients or other factors from damaged KCs.

These studies have revealed a critical role for Myd88 signaling within KCs in orchestrating cutaneous inflammation induced by epicutaneous *S. aureus* infection. In mice with deletion of Myd88 in KCs, there was reduction of skin inflammation which was associated with impaired production of IL-1 $\alpha$  and IL-36 $\alpha$  by KCs. Studies *in vivo* and *in vitro* revealed that IL-1 $\alpha$  and IL-36 $\alpha$  expression is enhanced by *S. aureus* stimulation and this is impaired in *Myd88*<sup>-/-</sup> KCs. Furthermore, induction of IL-1 $\alpha$  and IL-36 $\alpha$  by *S. aureus* was reduced by IL-1R deficiency and IL-36R neutralization, respectively. These results suggest that IL-1 $\alpha$  and IL-36 $\alpha$  act in a positive feedback loop that regulates their own expression via Myd88 signaling in KCs. These studies do not rule out a role for Myd88 on cells other than KCs to regulate the inflammatory response in the skin. IL-1R and IL-36R are expressed on immune cells and regulate the differentiation of IL-17-producing immune cells including  $\gamma\delta$  T cells, Th17 cells and ILC3 (Klose and Artis, 2016; Tortola et al., 2012; Vigne et al., 2011). Therefore, it is likely that Myd88 also acts critically on immune cells via IL-1R and IL-36R stimulation to regulate the induction of IL-17-producing cells in response to *S. aureus* epidermal infection. The phenotype of *Myd88*<sup>-/-</sup> mice is in contrast to that observed in the intradermal *S. aureus* inoculation model in which Myd88 deficiency is associated with increased pathogen loads and tissue pathology (Miller et al., 2006). The opposite roles of Myd88 in the two models suggest a different function of the immune system in the presence and absence of pathogen invasion. In the epicutaneous model, the epidermal barrier is not

physically breached, and epidermal thickening and the recruitment of neutrophils are induced via Myd88 function to prevent pathogen invasion. In contrast to the role of Myd88 signaling in sensing pathogen on the epidermal surface in the epicutaneous model, in the dermal/subcutaneous model Myd88 signaling appears more critical in promoting killing of *S. aureus* by immune cells within in the dermis and subcutaneous tissues (Miller et al., 2006).

Our findings may have relevance to the inflammatory response associated with some forms of dermatitis in humans. Over 90% of atopic dermatitis (AD) patients are colonized in the lesional epidermis by *S. aureus*, which is increased during disease flares (Kong et al., 2012; Rudikoff and Lebowitz, 1998). In adult AD, lesional skin has been associated with Th2, Th22 and Th17 immune polarization, but strong Th17 polarization is characteristic of new-onset pediatric AD (Esaki et al., 2016). Previous work revealed the expression of *S. aureus* Agr virulence factors that produce PSMs in the lesional skin in AD (Nakamura et al., 2013). Furthermore,  $\delta$ -toxin promoted allergic skin disease through the activation of mast cells that induces Th2 type inflammation in the epicutaneous *S. aureus* model (Nakamura et al., 2013). Together, these results indicate that different PSMs contribute to *S. aureus*-induced skin IL-17-driven inflammation via different mechanisms. However, a role for PSM $\alpha$ -induced IL-1 $\alpha$  and IL-36 production in the pathogenesis of AD remains to be investigated. Although there is no direct evidence of *S. aureus* colonization in psoriasis, both psoriasis vulgaris and generalized pustular psoriasis are associated with increased production of IL-1 and IL-36 cytokines (D'Erme et al., 2015; Johnston et al., 2016). The importance of IL-36 in generalized pustular psoriasis is highlighted by the observation that missense loss-of-function mutations of the IL-36R antagonist leading to unrestrained IL-36 activity, which is associated with the disease (Marrakchi et al., 2011). Furthermore, neutralization of IL-17 is highly effective in the treatment of psoriasis (McInnes et al., 2015; Papp et al., 2012). Thus, IL-17 appears to promote protective immunity against pathogens, but if its production is excessive can also contribute to inflammatory disease. Our observations suggest that identifying pathogenic stimuli that trigger KC damage would help unravel the mechanisms underlying the induction of pathogenic IL-17 responses often associated with psoriasis.

## STAR METHODS

### KEY RESOURCES TABLE

REAGENT or RESOURCE	SOURCE	IDENTIFIER
Antibodies		
Armenian hamster monoclonal anti-IL-1 $\alpha$ (clone ALF-161)	BioXCell	Cat# BE0243
Armenian hamster polyclonal IgG	BioXCell	Cat# BE0091
Goat polyclonal anti-IL-36 $\alpha$	R&D Systems	Cat# AF2297; RRID: AB_355216
Mouse monoclonal anti- <i>S. aureus</i> (clone 704)	Abcam	Cat# ab37644; RRID: AB_778082
Rat monoclonal anti-CD16/32 (clone 93)	BioLegend	Cat# 101302; RRID: AB_312801
Rat monoclonal anti-CD90 (clone T24/31)	BioXCell	Cat# BE0212
Rat monoclonal anti-IL-36 receptor (clone M616)	Amgen	MTA



REAGENT or RESOURCE	SOURCE	IDENTIFIER
Rat monoclonal IgG2a isotype control (clone 2A3)	BioXCell	Cat# BE0089
Rat monoclonal IgG2b isotype control (clone LTF-2)	BioXCell	Cat# BE0090
Alexa Fluor 488 rabbit polyclonal anti-goat IgG	Life Technologies	Cat# A11078; RRID: AB_10584486
Alexa Fluor 647 goat polyclonal anti-mouse IgG	Invitrogen	Cat# A-21463; RRID: AB_2535869
APC anti-CD45	eBioscience	Cat# 17-0451-82; RRID: AB_469392
APC anti-IL-17A	eBioscience	Cat# 17-7177-81; RRID: AB_763580
Brilliant Violet 421 anti-CD3e	BioLegend	Cat# 100341; RRID: AB_2562556
Brilliant Violet 421 anti- $\gamma\delta$ TCR	BioLegend	Cat# 118120; RRID: AB_2562566
FITC anti-CD90.2	eBioscience	Cat# 11-0902-85; RRID: AB_465154
FITC anti-GM-CSF	BioLegend	Cat# 505403; RRID: AB_315379
Pacific Blue anti-CD90.2	BioLegend	Cat# 140305; RRID: AB_10645335
PE anti-B220	eBioscience	Cat# 12-0452-83; RRID: AB_465671
PE anti-CD11b	BioLegend	Cat# 101208; RRID: AB_312791
PE anti-CD11c	BioLegend	Cat# 117307; RRID: AB_313776
PE anti- $\gamma\delta$ TCR	eBioscience	Cat# 12-5711-81; RRID: AB_465934
PE anti-Gr1	BD Biosciences	Cat# 553128
PE anti-IFN- $\gamma$	Thermo Fisher Scientific	Cat# RM9004; RRID: AB_10376293
PE anti-IL-1 $\alpha$	BioLegend	Cat# 503203; RRID: AB_315281
PE anti-IL-17F	eBioscience	Cat# 12-7471-80; RRID: AB_1210742
PE anti-NK1.1	BioLegend	Cat# 108707; RRID: AB_313394
PECy7 anti-CD45	BioLegend	Cat# 103113; RRID: AB_312978
PerCP5.5 Armenian hamster IgG	BioLegend	Cat# 400931
PerCP5.5 anti-CD45	BD Biosciences	Cat# 561869; RRID: AB_394003
PerCP5.5 anti-TCR $\beta$	BioLegend	Cat# 109227; RRID: AB_1575176
PerCP-eFluor 710 anti-IL-22	eBioscience	Cat# 46-7221-80; RRID: AB_10598646
Bacterial and Virus Strains		
<i>Staphylococcus aureus</i> LAC (USA300) wild-type	Dr. Michael Otto (Wang et al., 2007)	N/A
<i>Staphylococcus aureus</i> LAC (USA300) <i>psma</i>	Dr. Michael Otto (Wang et al., 2007)	N/A
<i>Staphylococcus aureus</i> LAC (USA300) <i>psm<math>\beta</math></i>	Dr. Michael Otto (Wang et al., 2007)	N/A
<i>Staphylococcus aureus</i> LAC (USA300) <i>psma</i> with plasmid pTX <i>psma</i>	Dr. Michael Otto (Wang et al., 2007)	N/A
<i>Staphylococcus aureus</i> LAC (USA300) <i>psma</i> with plasmid pTX <i>16</i>	Dr. Michael Otto (Wang et al., 2007)	N/A
Biological Samples		
Human primary keratinocytes obtained from hair follicle	Chiba University Hospital (Nakano et al., 2016)	N/A
Chemicals, Peptides, and Recombinant Proteins		

REAGENT or RESOURCE	SOURCE	IDENTIFIER
Accutase Cell Detachment Solution	CELLnTEC	Cat# CnT-ACCUTASE-100
Blocking One	Nacalai Tesque	Cat# 03953-95
Brefeldin A	BD Biosciences	Cat# 555029
Collagenase type 2	Worthington	Cat# LS004176
Dispase	CELLnTEC	Cat# CnT-DNP-10
Dispase II	Sigma-Aldrich	Cat# D4693
DNase I	Sigma-Aldrich	Cat# DN25
Fixable Viability Dye eFluor 780	eBioscience	Cat# 65-0865-14
Fluorescent mounting medium	Dako	Cat# S3023
Hoechst 33342	Invitrogen	Cat# H3570
Human IL-1 receptor antagonist	Wako	Cat# 093-05991
Hyaluronidase	Sigma-Aldrich	Cat# H3506
Ionomycin	Sigma-Aldrich	Cat# I9657
Keratinocyte Growth Medium 2	PromoCell	Cat# C20011
Mannitol salt agar	Nissui	Cat# 05236
PCT Epidermal Keratinocyte Medium	CELLnTEC	Cat# CnT-07
Percoll	GE Healthcare	Cat# 17-0891-01
Phorbol 12-myristate 13-acetate	Sigma-Aldrich	Cat# 79346
Proteinase-inhibitor	Thermo Fisher Scientific	Cat# 78430
Recombinant formylated phenol-soluble modulin $\alpha$ 3	Invitrogen	Cat# N/A
RIPA buffer	Wako	Cat# 182-02451
Target retrieval solution pH 9	Dako	Cat# S2031
Critical Commercial Assays		
CytoTox96® Non-Radioactive Cytotoxicity Assay	Promega	Cat# G1780
Human IL-1 $\alpha$ ELISA kit	R&D Systems	Cat# DLA50
Mouse IL-1 $\alpha$ ELISA kit	eBioscience	Cat# 88-5019
Mouse IL-17A Flex set	BD Biosciences	Cat# 560283
Mouse IL-17F Flex set	BD Biosciences	Cat# 562174
Experimental Models: Cell Lines		
Murine primary keratinocyte obtained from C57BL/6J mice	In this paper	N/A
Murine primary keratinocyte obtained from <i>Il1r<sup>-/-</sup></i> mice	In this paper	N/A
Murine primary keratinocyte obtained from <i>Myd88<sup>-/-</sup></i> mice	In this paper	N/A
Experimental Models: Organisms/Strains		
Mouse: C57BL/6J	The Jackson Laboratory (CLEA Japan)	JAX: 000664
Mouse: <i>Il1r<sup>-/-</sup></i> ; B6.129S7- <i>Il1r1<sup>tm1Imx</sup></i> J	The Jackson Laboratory	JAX: 003245
Mouse: <i>Il1<math>\beta</math><sup>-/-</sup></i>	Dr. Yoichiro Iwakura (Horai et al., 1998)	MGI: 2157396

REAGENT or RESOURCE	SOURCE	IDENTIFIER
Mouse: <i>Il17a<sup>-/-</sup>f<sup>-/-</sup></i>	Dr. Shinobu Saijo (Ishigame et al., 2009)	MGI: 3830057
Mouse: <i>Il18<sup>-/-</sup></i>	Dr. Shizuo Akira (Takeda et al., 1998)	MGI: 2136769
Mouse: <i>Il22<sup>-/-</sup></i>	Genentech (Zheng et al., 2007)	MGI: 3699310
Mouse: <i>K14-Cre</i> ; B6N.Cg-Tg(KRT14-cre)1Amc/J	The Jackson Laboratory	JAX: 018964
Mouse: <i>Myd88<sup>-/-</sup></i>	Dr. Shizuo Akira (Adachi et al., 1998)	MGI: 2385681
Mouse: <i>Myd88<sup>fl/fl</sup></i>	Dr. Xiaoxia Li (Hou et al., 2008)	MTA
Mouse: <i>Tcrδ<sup>-/-</sup></i> ; B6.129P2- <i>Tcrδ<sup>tm1Mom</sup>/J</i>	The Jackson Laboratory	JAX: 002120
Mouse: <i>Tlr2<sup>-/-</sup>4<sup>-/-</sup></i>	Dr. Shizuo Akira (Hoshino et al., 1999, Takeuchi et al., 1999)	MGI: 2178675
Recombinant DNA		
pTX <i>psma</i>	Wang et al., 2007	N/A
pTX <i>I6</i>	Wang et al., 2007	N/A
Software and Algorithms		
Axio vision	Zeiss	<a href="https://www.zeiss.com/microscopy/int/products/microscope-software">https://www.zeiss.com/microscopy/int/products/microscope-software</a>
BZ-H3A	Keyence	N/A
FCAP Array™ Software	BD Bioscience	<a href="https://www.bdbiosciences.com/documents/BD_FCAP_Array_Software">https://www.bdbiosciences.com/documents/BD_FCAP_Array_Software</a>
FlowJo	N/A	<a href="https://www.flowjo.com">https://www.flowjo.com</a>
Gen5™	BioTek	<a href="https://www.biotek.com/products/software-robotics-software/gen5-m">https://www.biotek.com/products/software-robotics-software/gen5-m</a>
Prism (GraphPad Software)	N/A	<a href="https://www.graphpad.com">https://www.graphpad.com</a>

## CONTACT FOR REAGENT AND RESOURCING SHARING

Further information and requests for resources and reagents should be directed to and will be fulfilled by the Lead Contact, Gabriel Nunez (gabriel.nunez@umich.edu).

## EXPERIMENTAL MODELS AND SUBJECTS DETAILS

**Animals**—C57BL/6 mice were purchased from CLEA Co. (Tokyo, Japan) or the Jackson Laboratory and expanded in our mouse Facility. *K14-Cre* and *Tcrδ<sup>-/-</sup>* were purchased from the Jackson Laboratory. *Tlr2<sup>-/-</sup>4<sup>-/-</sup>*, *Myd88<sup>-/-</sup>*, *Il1r<sup>-/-</sup>*, *Il1β<sup>-/-</sup>*, *Il18<sup>-/-</sup>* and *Il17a<sup>-/-</sup>f<sup>-/-</sup>* mice on C57BL/6 background have been described previously (Adachi et al., 1998; Franchi et al., 2012; Horai et al., 1998; Hoshino et al., 1999; Ishigame et al., 2009; Takeda et al., 1998; Takeuchi et al., 1999). *Myd88<sup>fl/fl</sup>* mice on C57BL/6 background were a gift from Dr. Xiaoxia Li (The Cleveland Clinic)(Hou et al., 2008). *Il22<sup>-/-</sup>* mice on C57BL/6 background were obtained from Genentech. All mice were maintained under specific pathogen-free conditions and were used at 8 to 12 weeks of age. Female mice were used in the majority of the experiments. All animal studies were performed according to approved protocols by Chiba University or the University of Michigan Review Board for Animal Care.

**Isolation of murine primary keratinocytes**—Skins isolated from neonatal (day 1–3 after birth) WT, *Il1r<sup>-/-</sup>* and *Myd88<sup>-/-</sup>* mice were treated with 5 mg/ml dispase (CELLnTEC) overnight and then separated into dermis and epidermis. The epidermis sheets were treated with accutase (CELLnTEC) for 30 min and single-cell suspensions prepared from the epidermal sheets were cultured in CnT-07 medium (CELLnTEC) for 5–6 days. After confluency, terminal differentiation of KCs was induced by addition of 1.2 mM CaCl<sub>2</sub> for the last 2 days. To block IL-36R, mouse KCs were treated with anti-IL-36R Ab (30 µg/ml) or its isotype control Ab (clone: 2A3)(BioXCell) before addition of CaCl<sub>2</sub>.

**Preparation of human primary keratinocytes**—Human primary KCs were established as previously described (Nakano et al., 2016). 1×10<sup>4</sup> cells in 24-well plate were cultured in Keratinocyte Growth Medium 2 (PromoCell) for 4–7 days. After confluency, terminal differentiation of KCs was induced by an addition of 1.8 mM CaCl<sub>2</sub> for last 2 days. To block human IL-1 receptor, human primary KCs were treated with human IL-1 receptor antagonist, Anakinra (50 µg/ml) (Wako), every 12 hrs from 48 hrs before stimulation. The collection of skin samples and the use of primary KC samples was approved by the ethics committee of Chiba University Graduate School of Medicine (No. 519).

## METHOD DETAILS

**Antibody treatment**—For antibody-mediated depletion, antibodies were purchased from BioXCell. To deplete ILCs, mice were treated with anti-CD90 antibody (200 µg) (clone: T24/31) subcutaneously on day -4, -2, 0, 2, 4, and 6 of *S. aureus* infection. Mice were treated with anti-IL-1α antibody (100 µg) (clone: ALF-161) subcutaneously on a daily base starting from day -1 of infection. To neutralize IL-36R, mice were injected intradermally on day 0 and intraperitoneally on day 1, 3 and 5 with an anti-IL36R Mab (50 µg) (clone: M616) provided by Amgen.

**Cell isolation and flow cytometric analysis**—For isolation of skin mononuclear cells, skin tissues were treated with 0.5% dispase II (Sigma) and then digested with 1.6 mg/ml collagenase type 2 (Worthington), 100 µg/ml deoxyribonuclease I (DNase I; Sigma) and 1.2 mg/ml hyaluronidase (Sigma). The cells were resuspended on a Percoll gradient (75%/40%) (GE Healthcare) and centrifuged at 2000 rpm for 20 min at 25°C. Single-cell suspensions were stimulated with 100 ng/ml phorbol 12-myristate 13-acetate (PMA; Sigma) plus 1 µM ionomycin (Sigma) for 4 hrs in the presence of brefeldin A (BD Biosciences) and then stained with the following fluorochrome-conjugated antibodies purchased from BD Biosciences, Biolegend, or eBioscience: Allophycocyanin (APC)-conjugated anti-CD45 (30-F11); brilliant violet 421-conjugated anti-CD3e (145-2C11) and anti-γδ TCR (GL3); Fixable Viability Dye eFluor 780; fluorescein isothiocyanate (FITC)-conjugated anti-CD90.2 (53-2.1); pacific blue-conjugated anti-CD90.2 (53-2.1); peridinin chlorophyll protein complex-cyanin 5.5 (PerCP5.5)-conjugated Armenian Hamster IgG (HTK888), anti-CD45 (30-F11) and anti-TCRβ (H57-597); phycoerythrin (PE)-conjugated anti-B220 (RA-6B2), anti-CD11b (M1/70), anti-CD11c (HL3), anti-γδ TCR (GL3), anti-Gr1 (RB6-8C5) and anti-NK1.1 (PK136) ; PE-Cy7 conjugated anti-CD45 (30-F11). The cells were fixed and permeabilized with Cytotfix/Cytoperm (BD Biosciences) before intracellular staining with APC-conjugated anti-IL-17A (TC11-18H10), FITC-conjugated anti-GM-CSF

(MP1-22E9), PerCP-eFluor710-conjugated anti-IL-22 (1H8PWSR) and PE-conjugated anti-IFN- $\gamma$  (XMG1.2) and anti-IL-17F (eBio18F10) and then analyzed on a LSRII flow cytometer (BD Biosciences).

**Cytometric bead assay**—Supernatants from crude suspension of epidermis and dermis were collected from colonized skin and then protein level of IL-17A and IL-17F was measured by BD™ CBA Flex Sets according to the manufacturer's instructions (BD Biosciences). The results were generated using CBA analysis software (BD Bioscience-PharMingen).

**Cytotoxicity Assay**—Cytotoxicity were measured by LDH release assay with CytoTox 96® Non-Radioactive Cytotoxicity Assay (Promega). Primary KCs were stimulated with various *S. aureus* culture supernatants and LDH release assay was performed according to manufacturers' instructions.

**Enzyme-linked immunosorbent assay**—Mouse IL-1 $\alpha$  was detected with IL-1 alpha ELISA Ready-Set-Go! Kit (eBioscience). Purified IL-1 $\alpha$  capturing antibody was added to a coated Nunc-Immuno™ plate (Thermo scientific). After blocking with blocking buffer provided in the kit, supernatants from primary KCs were added and the cells were incubated at room temperature for 2 h. The binding of IL-1 $\alpha$  was detected by HRP-conjugated detection antibody and TMB solution (eBioscience). Human IL-1 $\alpha$  was detected with Quantikine® ELISA Human IL-1 $\alpha$ /IL-1F1 Immunoassay (R&D). IL-1 $\alpha$  measurement was performed according to manufacturers' instructions.

**Western blotting**—Supernatants were concentrated with an Amicon® Ultra-0.5 centrifuge filter device. Primary KCs were lysed in the presence of proteinase-inhibitor (Thermo Scientific) and RIPA buffer (Wako) was added. The eluted samples were separated on 15% SDS-PAGE, transferred to polyvinylidene difluoride membranes by electrophoresis and then analyzed by immunoblot with anti-mouse IL-36 $\alpha$  antibody (R&D systems) followed by HRP-conjugated secondary antibody.

**Immunofluorescent staining**—Sections of skins fixed in 10% paraformaldehyde were treated with Target Retrieval Solution pH 9 (Dako) for IL-36 $\alpha$  immunofluorescent staining, and frozen sections of skins were fixed with acetone for IL-1 $\alpha$  immunofluorescent staining. The skin sections were treated with polyclonal antibodies against mouse IL-36 $\alpha$  (R&D systems) and *S. aureus* (abcam) at 4°C overnight and then stained with Alexa Fluor 488-labeled anti-goat IgG antibodies (Life technologies) and Alexa Fluor 647 anti-mouse IgG antibodies (Invitrogen), respectively. For IL-1 $\alpha$  and nuclear staining, PE-conjugated anti-IL-1 $\alpha$  (ALF-161, Biolegend) and Hoechst (Invitrogen) were used, respectively. Images of stained sections were viewed with fluorescence microscope Axio Observer (Carl Zeiss) for IL-36 $\alpha$  and BZ-X700 (Keyence) for IL-1 $\alpha$ .

***S. aureus* colonization**—The methicillin-resistant *Staphylococcus aureus* strain USA300 (LAC) and the isogenic *psma*, *psma* pTX 16, *psma* pTX a and *psm* $\beta$  mutant strains have been described (Wang et al., 2007). For colonization, bacteria were grown for 4 hrs in tryptic soy broth with shaking at 37°C. Mice were colonized on the shaved dorsal skin of

mice by applying a 1 cm<sup>2</sup> sterile gauze containing 1 × 10<sup>8</sup> CFUs of *S. aureus* which was covered with occlusive plastic dressing. In some experiments, mice were intradermally injected with 1 × 10<sup>6</sup> CFUs of *S. aureus*. To determine bacterial numbers in the colonized skin, skin was collected from individual mice, homogenized in cold PBS and plated at serial dilution onto Mannitol-salt agar containing 10% egg yolk. The number of CFU was determined after 24 hrs of incubation at 37°C. Mice were sacrificed on day 7 day after colonization, and skins were assessed in a blinded fashion using a scoring system described previously (Nakamura et al., 2013). Briefly, 4 points were used to denote the severity of erythema (0, none; 1, mild; 2, moderate; 3, severe), scaling (0, none; 1, mild; 2, moderate; 3, severe), erosion (0, none; 1, mild; 2, moderate; 3, severe), edema (0, none; 1, mild; 2, moderate; 3, severe), and thickness (0, none; 1, mild; 2, moderate; 3, severe). Skin samples were fixed in 10% formalin and processed for HE staining or frozen sections were obtained for immunohistochemistry.

## QUANTIFICATION AND STATISTICAL ANALYSES

Statistical analyses were performed using GraphPad Prism software version 5.0 (GraphPad Software Inc.). Differences between two groups were evaluated using Student's t test (parametric) or Mann-Whitney U test (non-parametric). For multiple comparisons, statistical analysis was performed using one-way ANOVA (parametric) or Kruskal-Wallis test (nonparametric), and then Bonferroni test for parametric samples, or Dunn's test for nonparametric samples as a post-hoc test. Differences at P<0.05 were considered significant.

## Supplementary Material

Refer to Web version on PubMed Central for supplementary material.

## Acknowledgments

The authors thank the University of Michigan Flow Cytometry Core for Flow cytometry analysis, A. Oikawa in Chiba University for histology analysis, N. Saito in Chiba University for Enzyme-linked immunosorbent assay analysis and Melody Zeng for review of the manuscript. This work was supported by JSPS KAKENHI; Grant Number 26713038 (Y.N.), 16H06252 (Y.N.), the Naito Foundation (Y.N.), the Uehara Memorial Foundation (M.M.), Mochida Memorial Foundation for Medical and Pharmaceutical Research (M.M.) and NIH grant AR069303 (G.N.). Y.N. and S.N. were supported by Institute for Global Prominent Research, Chiba University. S.N. was supported by the Leading Graduate School Program of Chiba University (Nurture of Creative Research Leaders in Immune System Regulation and Innovative Therapeutics). M.O. was supported by the Intramural Research Program of the National Institute of Allergy and Infectious Diseases, US National Institutes of Health (grant number ZIA AI000904-16).

## References

- Adachi O, Kawai T, Takeda K, Matsumoto M, Tsutsui H, Sakagami M, Nakanishi K, Akira S. Targeted disruption of the MyD88 gene results in loss of IL-1- and IL-18-mediated function. *Immunity*. 1998; 9:143–150. [PubMed: 9697844]
- Balsubramanian D, Harper L, Shopsis B, Torres VJ. *Staphylococcus aureus* pathogenesis in diverse host environments. *Pathog Dis*. 2017
- Bikle DD, Xie Z, Tu CL. Calcium regulation of keratinocyte differentiation. *Expert Rev Endocrinol Metab*. 2012; 7:461–472. [PubMed: 23144648]
- Cheung GY, Joo HS, Chatterjee SS, Otto M. Phenol-soluble modulins--critical determinants of staphylococcal virulence. *FEMS Microbiol Rev*. 2014; 38:698–719. [PubMed: 24372362]



- Cheung GY, Rigby K, Wang R, Queck SY, Braughton KR, Whitney AR, Teintze M, DeLeo FR, Otto M. Staphylococcus epidermidis strategies to avoid killing by human neutrophils. *PLoS Pathog.* 2010; 6:e1001133. [PubMed: 20949069]
- D'Erme AM, Wilsmann-Theis D, Wagenpfeil J, Holzel M, Ferring-Schmitt S, Sternberg S, Wittmann M, Peters B, Bosio A, Bieber T, et al. IL-36gamma (IL-1F9) is a biomarker for psoriasis skin lesions. *J Invest Dermatol.* 2015; 135:1025–1032. [PubMed: 25525775]
- Esaki H, Brunner PM, Renert-Yuval Y, Czarnowicki T, Huynh T, Tran G, Lyon S, Rodriguez G, Immaneni S, Johnson DB, et al. Early-onset pediatric atopic dermatitis is TH2 but also TH17 polarized in skin. *J Allergy Clin Immunol.* 2016; 138:1639–1651. [PubMed: 27671162]
- Franchi L, Kamada N, Nakamura Y, Burberry A, Kuffa P, Suzuki S, Shaw MH, Kim YG, Nunez G. NLR4-driven production of IL-1beta discriminates between pathogenic and commensal bacteria and promotes host intestinal defense. *Nat Immunol.* 2012; 13:449–456. [PubMed: 22484733]
- Gresnigt MS, van de Veerdonk FL. Biology of IL-36 cytokines and their role in disease. *Semin Immunol.* 2013; 25:458–465. [PubMed: 24355486]
- Horai R, Asano M, Sudo K, Kanuka H, Suzuki M, Nishihara M, Takahashi M, Iwakura Y. Production of mice deficient in genes for interleukin (IL)-1alpha, IL-1beta, IL-1alpha/beta, and IL-1 receptor antagonist shows that IL-1beta is crucial in turpentine-induced fever development and glucocorticoid secretion. *J Exp Med.* 1998; 187:1463–1475. [PubMed: 9565638]
- Hoshino K, Takeuchi O, Kawai T, Sanjo H, Ogawa T, Takeda Y, Takeda K, Akira S. Cutting edge: Toll-like receptor 4 (TLR4)-deficient mice are hyporesponsive to lipopolysaccharide: evidence for TLR4 as the Lps gene product. *J Immunol.* 1999; 162:3749–3752. [PubMed: 10201887]
- Hou B, Reizis B, DeFranco AL. Toll-like receptors activate innate and adaptive immunity by using dendritic cell-intrinsic and -extrinsic mechanisms. *Immunity.* 2008; 29:272–282. [PubMed: 18656388]
- Ishigame H, Kakuta S, Nagai T, Kadoki M, Nambu A, Komiyama Y, Fujikado N, Tanahashi Y, Akitsu A, Kotaki H, et al. Differential roles of interleukin-17A and -17F in host defense against mucocutaneous bacterial infection and allergic responses. *Immunity.* 2009; 30:108–119. [PubMed: 19144317]
- Johnston A, Xing X, Wolterink L, Barnes DH, Yin Z, Reingold L, Kahlenberg JM, Harms PW, Gudjonsson JE. IL-1 and IL-36 are dominant cytokines in generalized pustular psoriasis. *J Allergy Clin Immunol.* 2016
- Kennedy-Crispin M, Billick E, Mitsui H, Gulati N, Fujita H, Gilleaudeau P, Sullivan-Whalen M, Johnson-Huang LM, Suarez-Farinas M, Krueger JG. Human keratinocytes' response to injury upregulates CCL20 and other genes linking innate and adaptive immunity. *J Invest Dermatol.* 2012; 132:105–113. [PubMed: 21881590]
- Klose CS, Artis D. Innate lymphoid cells as regulators of immunity, inflammation and tissue homeostasis. *Nat Immunol.* 2016; 17:765–774. [PubMed: 27328006]
- Kong HH, Oh J, Deming C, Conlan S, Grice EA, Beatson MA, Nomicos E, Polley EC, Komarow HD, Program NCS, et al. Temporal shifts in the skin microbiome associated with disease flares and treatment in children with atopic dermatitis. *Genome Res.* 2012; 22:850–859. [PubMed: 22310478]
- Kretschmer D, Gleske AK, Rautenberg M, Wang R, Koberle M, Bohn E, Schoneberg T, Rabet MJ, Boulay F, Klebanoff SJ, et al. Human formyl peptide receptor 2 senses highly pathogenic Staphylococcus aureus. *Cell Host Microbe.* 2010; 7:463–473. [PubMed: 20542250]
- Lowy FD. Staphylococcus aureus infections. *N Engl J Med.* 1998; 339:520–532. [PubMed: 9709046]
- Marrakchi S, Guigue P, Renshaw BR, Puel A, Pei XY, Fraitag S, Zribi J, Bal E, Cluzeau C, Chrabieh M, et al. Interleukin-36-receptor antagonist deficiency and generalized pustular psoriasis. *N Engl J Med.* 2011; 365:620–628. [PubMed: 21848462]
- McInnes IB, Mease PJ, Kirkham B, Kavanaugh A, Ritchlin CT, Rahman P, van der Heijde D, Landewe R, Conaghan PG, Gottlieb AB, et al. Secukinumab, a human anti-interleukin-17A monoclonal antibody, in patients with psoriatic arthritis (FUTURE 2): a randomised, double-blind, placebo-controlled, phase 3 trial. *Lancet.* 2015; 386:1137–1146. [PubMed: 26135703]
- Miller LS, O'Connell RM, Gutierrez MA, Pietras EM, Shahangian A, Gross CE, Thirumala A, Cheung AL, Cheng G, Modlin RL. MyD88 mediates neutrophil recruitment initiated by IL-1R but not

- TLR2 activation in immunity against *Staphylococcus aureus*. *Immunity*. 2006; 24:79–91. [PubMed: 16413925]
- Naik S, Bouladoux N, Linehan JL, Han SJ, Harrison OJ, Wilhelm C, Conlan S, Himmelfarb S, Byrd AL, Deming C, et al. Commensal-dendritic-cell interaction specifies a unique protective skin immune signature. *Nature*. 2015; 520:104–108. [PubMed: 25539086]
- Naik S, Bouladoux N, Wilhelm C, Molloy MJ, Salcedo R, Kastenmuller W, Deming C, Quinones M, Koo L, Conlan S, et al. Compartmentalized control of skin immunity by resident commensals. *Science*. 2012; 337:1115–1119. [PubMed: 22837383]
- Nakamura Y, Oscherwitz J, Cease KB, Chan SM, Munoz-Planillo R, Hasegawa M, Villaruz AE, Cheung GY, McGavin MJ, Travers JB, et al. *Staphylococcus delta*-toxin induces allergic skin disease by activating mast cells. *Nature*. 2013; 503:397–401. [PubMed: 24172897]
- Nakano M, Kamada N, Suehiro K, Oikawa A, Shibata C, Nakamura Y, Matsue H, Sasahara Y, Hosokawa H, Nakayama T, et al. Establishment of a new three-dimensional human epidermal model reconstructed from plucked hair follicle-derived keratinocytes. *Exp Dermatol*. 2016; 25:903–906. [PubMed: 27194575]
- Nestle FO, Di Meglio P, Qin JZ, Nickoloff BJ. Skin immune sentinels in health and disease. *Nat Rev Immunol*. 2009; 9:679–691. [PubMed: 19763149]
- Novick RP. Autoinduction and signal transduction in the regulation of staphylococcal virulence. *Mol Microbiol*. 2003; 48:1429–1449. [PubMed: 12791129]
- Novick RP, Geisinger E. Quorum sensing in staphylococci. *Annu Rev Genet*. 2008; 42:541–564. [PubMed: 18713030]
- Palomo J, Dietrich D, Martin P, Palmer G, Gabay C. The interleukin (IL)-1 cytokine family--Balance between agonists and antagonists in inflammatory diseases. *Cytokine*. 2015; 76:25–37. [PubMed: 26185894]
- Papp KA, Leonardi C, Menter A, Ortonne JP, Krueger JG, Kricorian G, Aras G, Li J, Russell CB, Thompson EH, et al. Brodalumab, an anti-interleukin-17-receptor antibody for psoriasis. *N Engl J Med*. 2012; 366:1181–1189. [PubMed: 22455412]
- Rider P, Voronov E, Dinarello CA, Apte RN, Cohen I. Alarmins: Feel the Stress. *J Immunol*. 2017; 198:1395–1402. [PubMed: 28167650]
- Rudikoff D, Leibold M. Atopic dermatitis. *Lancet*. 1998; 351:1715–1721. [PubMed: 9734903]
- Segre JA. Epidermal barrier formation and recovery in skin disorders. *J Clin Invest*. 2006; 116:1150–1158. [PubMed: 16670755]
- Sonnenberg GF, Fouser LA, Artis D. Border patrol: regulation of immunity, inflammation and tissue homeostasis at barrier surfaces by IL-22. *Nat Immunol*. 2011; 12:383–390. [PubMed: 21502992]
- Takeda K, Tsutsui H, Yoshimoto T, Adachi O, Yoshida N, Kishimoto T, Okamura H, Nakanishi K, Akira S. Defective NK cell activity and Th1 response in IL-18-deficient mice. *Immunity*. 1998; 8:383–390. [PubMed: 9529155]
- Takeuchi O, Akira S. MyD88 as a bottle neck in Toll/IL-1 signaling. *Curr Top Microbiol Immunol*. 2002; 270:155–167. [PubMed: 12467250]
- Takeuchi O, Hoshino K, Kawai T, Sanjo H, Takada H, Ogawa T, Takeda K, Akira S. Differential roles of TLR2 and TLR4 in recognition of gram-negative and gram-positive bacterial cell wall components. *Immunity*. 1999; 11:443–451. [PubMed: 10549626]
- Tortola L, Rosenwald E, Abel B, Blumberg H, Schafer M, Coyle AJ, Renaud JC, Werner S, Kisielow J, Kopf M. Psoriasisiform dermatitis is driven by IL-36-mediated DC-keratinocyte crosstalk. *J Clin Invest*. 2012; 122:3965–3976. [PubMed: 23064362]
- Towne JE, Garka KE, Renshaw BR, Virca GD, Sims JE. Interleukin (IL)-1F6, IL-1F8, and IL-1F9 signal through IL-1Rrp2 and IL-1RAcP to activate the pathway leading to NF-kappaB and MAPKs. *J Biol Chem*. 2004; 279:13677–13688. [PubMed: 14734551]
- Vigne S, Palmer G, Lamacchia C, Martin P, Talabot-Ayer D, Rodriguez E, Ronchi F, Sallusto F, Dinh H, Sims JE, et al. IL-36R ligands are potent regulators of dendritic and T cells. *Blood*. 2011; 118:5813–5823. [PubMed: 21860022]
- Villarino AV, Laurence A. IL-1 watches the watchmen. *Nat Immunol*. 2015; 16:226–227. [PubMed: 25689436]

- Wang R, Braughton KR, Kretschmer D, Bach TH, Queck SY, Li M, Kennedy AD, Dorward DW, Klebanoff SJ, Peschel A, et al. Identification of novel cytolytic peptides as key virulence determinants for community-associated MRSA. *Nat Med.* 2007; 13:1510–1514. [PubMed: 17994102]
- Yang D, de la Rosa G, Tewary P, Oppenheim JJ. Alarmins link neutrophils and dendritic cells. *Trends Immunol.* 2009; 30:531–537. [PubMed: 19699678]

Author Manuscript

Author Manuscript

Author Manuscript

Author Manuscript

**HIGHLIGHTS**

- *S. aureus* virulence factor PSM $\alpha$  induces the release of keratinocyte IL-1 $\alpha$  and IL-36 $\alpha$
- Myd88 signaling in keratinocytes is required for IL-1 $\alpha$  and IL-36 $\alpha$  production
- IL-1R and IL-36R signaling is critical for the induction of IL-17-producing cells.
- Mice deficient in IL17A/F show blunted *S. aureus*-induced skin inflammation.

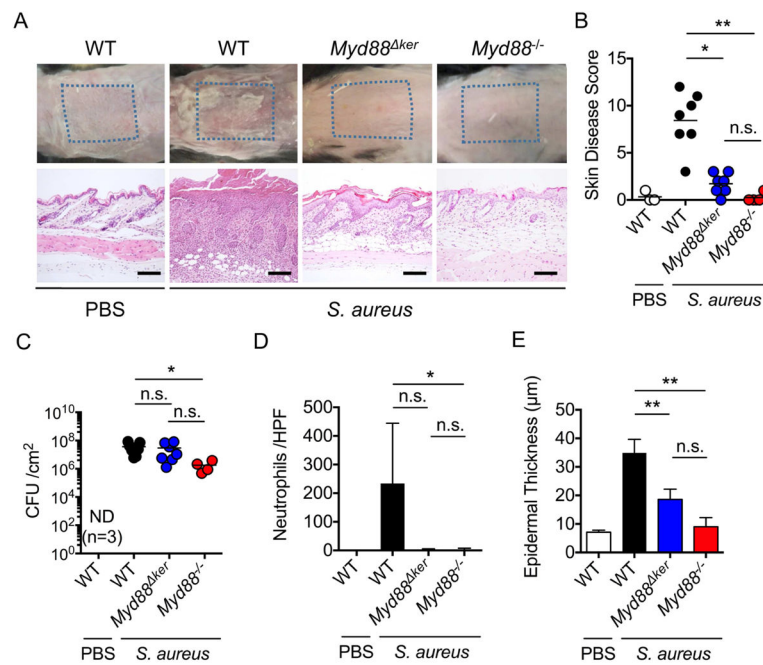


**Figure 1. Keratinocyte Myd88 is important for epicutaneous *S. aureus*-induced skin inflammation**

**A**, C57BL/6 (WT), *K14-CreMyd88<sup>fl/fl</sup>* (*Myd88<sup>ker</sup>*) and *Myd88<sup>-/-</sup>* mice were epicutaneously colonized with *S. aureus*. WT mice treated with PBS are shown for comparison. Representative macroscopic images and hematoxylin and eosin (HE)-stained skin sections 7 days after colonization (n=3 to 7 mice per group). Scale bars, 100 μm. **B**, Day 7 skin disease scores of WT, *Myd88<sup>ker</sup>* and *Myd88<sup>-/-</sup>* mice colonized with *S. aureus*. **C–E**, The number of *S. aureus* colony forming unit (CFU) (**C**), numbers of neutrophils per high power field (**D**), and epidermal thickness (**E**) in the skin of WT, *Myd88<sup>ker</sup>* and *Myd88<sup>-/-</sup>* mice 7 days after colonization with *S. aureus*. Each dot represents a mouse (B, C). Data are presented as mean ± SD (D, E). Results shown represent combined data of 2 independent experiments. ND; not detected, n.s.; not significant, \*P<0.05; \*\*P<0.01, by Kruskal-Wallis test.

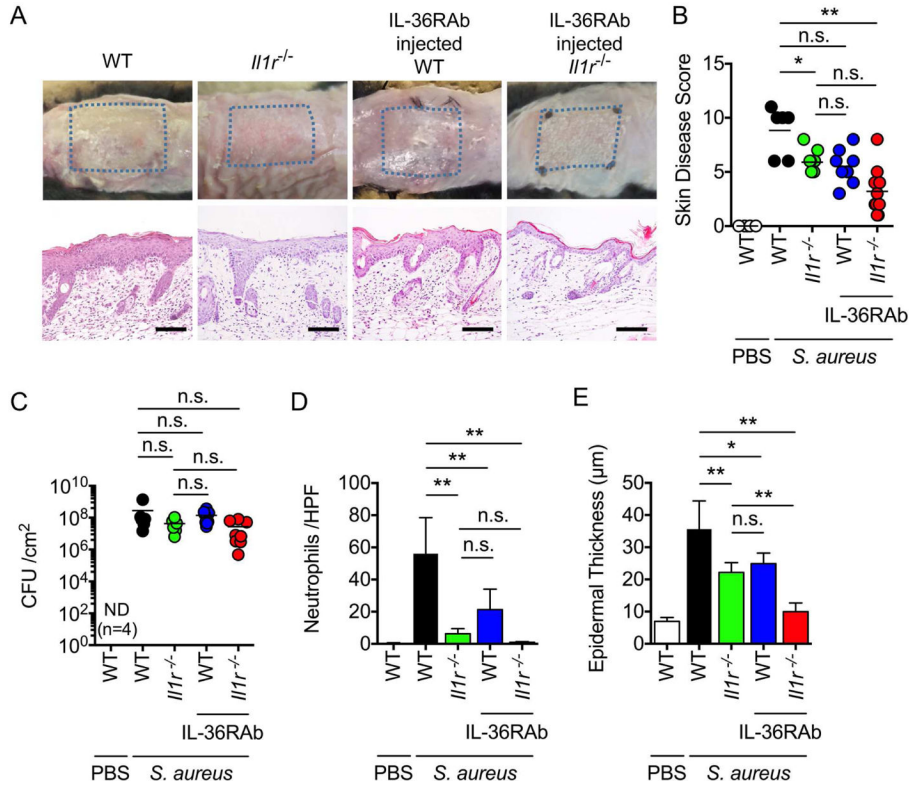


**Figure 2. Both IL-1R and IL-36R contribute to skin inflammation induced by epicutaneous *S. aureus* colonization**

**A**, WT, *Il1r*<sup>-/-</sup>, WT mice treated with IL-36R blocking antibody (IL-36RAb), and *Il1r*<sup>-/-</sup> mice treated with IL-36RAb were epicutaneously colonized with *S. aureus* for 7 days. Representative macroscopic images and HE-stained skin sections of mice colonized with *S. aureus* or treated with PBS (n=4 to 8 mice per group). Scale bars, 100 µm. **B–E**, Day 7 skin disease scores (**B**), *S. aureus* CFU in the skin (**C**), the number of neutrophils in the skin (**D**) and epidermal thickness (**E**) of WT, *Il1r*<sup>-/-</sup>, WT mice treated with IL-36RAb, and *Il1r*<sup>-/-</sup> mice treated with IL-36RAb (n=4 to 8 mice per group). WT mice treated with PBS are shown for comparison. Each dot represents a mouse (B, C). Data are presented as mean ± SD (D, E). Data represent combined results from 3 independent experiments. ND; not detected, n.s.; not significant, \*P<0.05 and \*\*P<0.01, by Kruskal-Wallis test (B, C) or by one-way ANOVA test with Bonferroni’s correction (D, E).



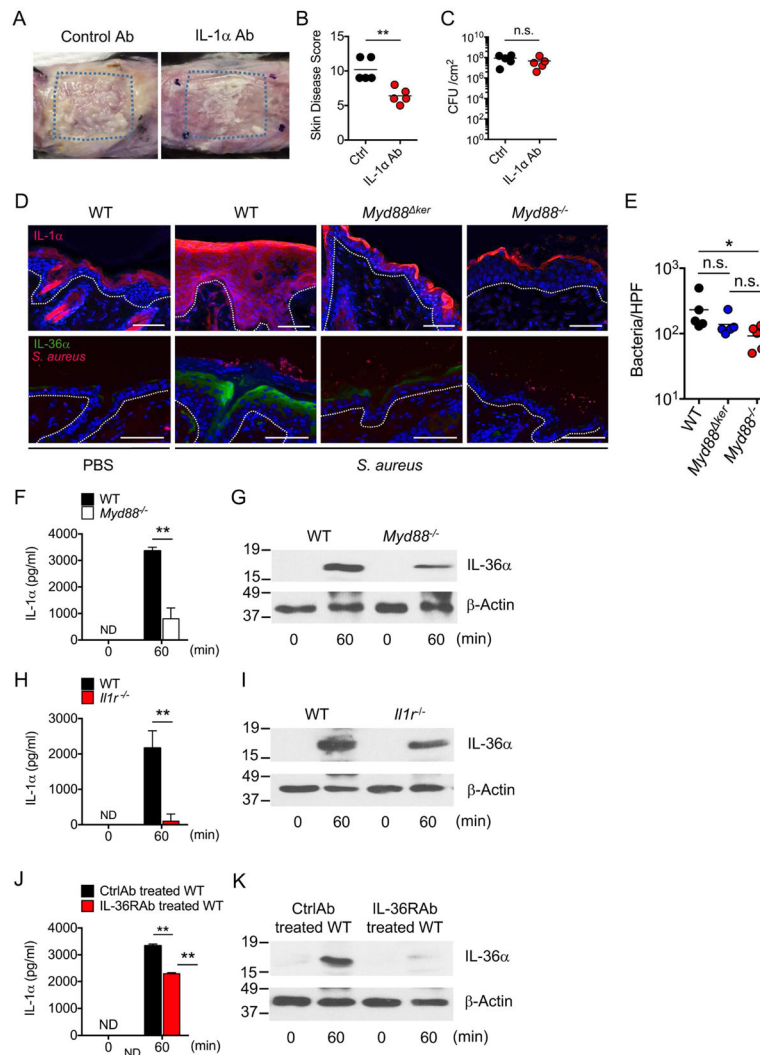


**Figure 3. IL-1 $\alpha$  and IL-36 $\alpha$  are induced by *S. aureus* via Myd88 signaling in keratinocytes**  
**A**, WT mice treated with IL-1 $\alpha$  blocking antibody (IL-1 $\alpha$ Ab) or isotype-matched control Ab were epicutaneously colonized with *S. aureus*. Representative macroscopic images of mice colonized with *S. aureus* (n=5 mice per group). **B–C**, Skin disease scores (**B**) and *S. aureus* CFU in the skin (**C**) of WT mice treated with IL-1 $\alpha$  Ab or control Ab. Each dot represents a mouse. **D**, Skin tissues of WT, and *Myd88<sup>ker</sup>* and *Myd88<sup>-/-</sup>* mice colonized with *S. aureus* or treated with PBS were stained with Hoechst stain (blue) and antibody against IL-1 $\alpha$  (red) or Hoechst stain (blue) and antibodies against *S. aureus* (red) and IL-36 $\alpha$  (green). Scale bars, 50  $\mu$ m. **E**, The numbers of *S. aureus* per high power field (HPF) are shown. Each dot represents average results from an individual mouse. Data are representative of 2 independent experiments. **F–K**, IL-1 $\alpha$  (**F**, **H**, **J**) and IL-36 $\alpha$  (**G**, **I**, **K**) release of differentiated primary KCs isolated from WT and *Myd88<sup>-/-</sup>* mice (**F**, **G**), WT and *Ilr1<sup>-/-</sup>* mice (**H**, **I**), or WT mice in the presence of anti-IL-36 neutralizing Mab or isotype-matched control Mab (**J**, **K**) and stimulated with culture supernatants of *S. aureus* for indicated time. IL-1 $\alpha$  and IL-36 $\alpha$  were detected by ELISA assay and immunoblotting, respectively.  $\beta$ -actin in whole cell lysates is shown as loading control. Data are presented as

mean±SD. Data are presented as mean ± SD. Data are representative of at least 2 independent experiments. ND; not detected, n.s.; not significant, \*P<0.05 and \*\*P<0.01, by unpaired two-tailed Mann-Whitney U test (B, C, F, H, J) or Kruskal-Wallis test (E).

Author Manuscript

Author Manuscript

Author Manuscript

Author Manuscript

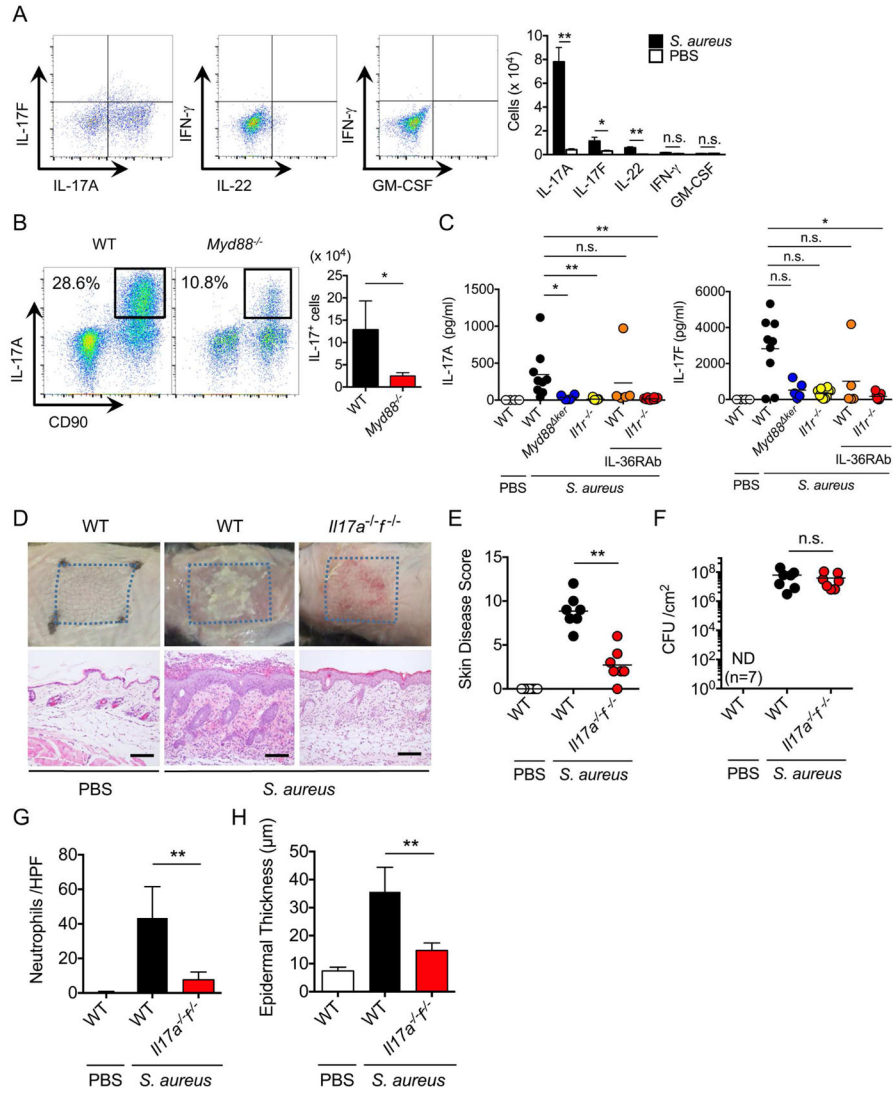


**Figure 4. IL-17 is critical for skin inflammation induced by epicutaneous *S. aureus* colonization**  
**A**, Production of IL-17A, IL-17F, IL-22, IFN- $\gamma$  and GM-CSF by skin cells isolated from WT mice colonized with *S. aureus* or treated with PBS. Intracellular cytokine production was assessed in gated CD45<sup>+</sup>CD90<sup>+</sup> cells on day 7 after pathogen colonization by flow cytometry. Representative flow cytometry profiles (left panels) and the number of cytokine-producing cells (right panel). Results in right panel represent mean  $\pm$  SD of 2 experiments.  
**B**, Production of IL-17A by CD45<sup>+</sup> cells in the skin of WT and *Myd88*<sup>-/-</sup> mice 7 days after epicutaneous infection. Representative flow cytometry profiles (left panels) and the number of IL-17A-producing cells (right panel). Results in right panel represent mean  $\pm$  SD of 2 experiments.  
**C**, IL-17A and IL-17F production in skin tissues of WT mice, *Myd88*<sup>ker</sup> mice, *Il1r*<sup>-/-</sup> mice, WT mice treated with IL-36Rab and *Il1r*<sup>-/-</sup> mice treated with IL-36Rab 7 days after pathogen colonization. WT mice treated with PBS are shown for comparison. Each dot represents a mouse. Data represent combined data of 3 independent experiments.  
**D** WT and *Il17a*<sup>-/-</sup> mice were epicutaneously colonized with *S. aureus* or treated with PBS. Representative macroscopic images and HE-stained skin sections 7 days after

colonization (n=7 mice per group). Scale bars, 100  $\mu\text{m}$ . **E–H**, Skin disease scores (**E**), *S. aureus* CFU in the skin (**F**), the numbers of neutrophils (**G**) and epidermal thickness (**H**) of WT and *Il17a<sup>-/-</sup>f<sup>-/-</sup>* mice colonized with *S. aureus*. WT mice treated with PBS are shown for comparison. Each dot represents a mouse (C, E, F). Data are presented as mean  $\pm$  SD (A, B, G, H). Results shown represent combined data of 3 independent experiments. ND; not detected, n.s.; not significant, \*P<0.05; \*\*P<0.01, by unpaired two-tailed Mann-Whitney U test (A, B, E, F, G, H) or Kruskal-Wallis test (C).

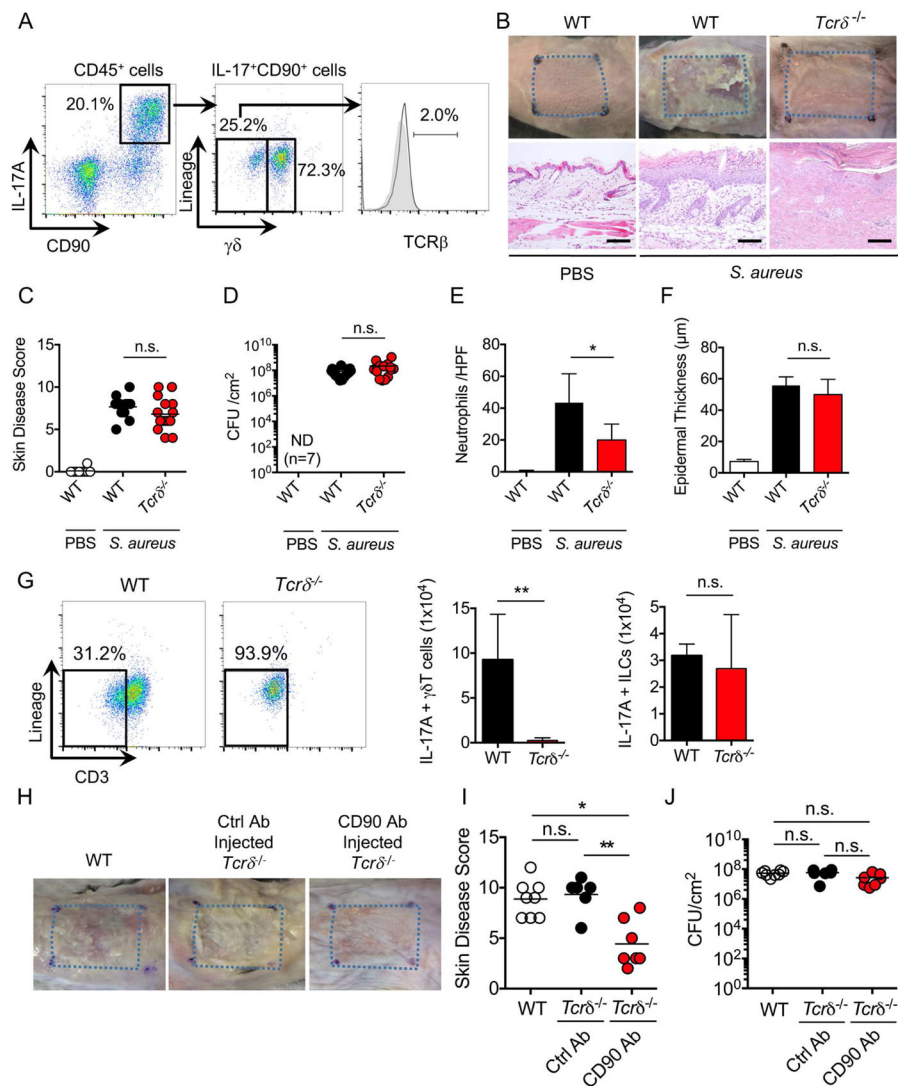


**Figure 5. Both  $\gamma\delta$  T cells and ILC3 contribute to skin inflammation after *S. aureus* colonization**  
**A**, IL-17A-producing  $\gamma\delta$  T cells, ILC3 and  $\alpha\beta$  T cells were evaluated by flow cytometric analysis after epicutaneous *S. aureus* colonization. Flow cytometric analysis of lineage (B220, CD11b, CD11c, Gr-1, NK1.1)-negative cells and  $\gamma\delta$  T cells was performed on gated CD45<sup>+</sup>CD90<sup>+</sup>IL-17A<sup>+</sup> skin cells. Data are representative of 3 independent experiments. **B**, WT and *Tcr* $\delta^{-/-}$  mice were epicutaneously colonized with *S. aureus*. WT mice treated with PBS are shown for comparison. Representative macroscopic images and HE-stained sections of mouse skin on day 7 after colonization (n=10 to 15 mice per group). Scale bars, 100  $\mu$ m. **C–E**, Day 7 skin disease scores (**C**), *S. aureus* CFU in the skin (**D**), neutrophil numbers in the skin (**E**) and epidermal thickening (**F**) of WT and *Tcr* $\delta^{-/-}$  mice colonized with *S. aureus*. Each dot represents a mouse (**C**, **D**). Data are presented as mean  $\pm$  SD (**E**, **F**). Results represent combined data of 4 independent experiments. **G**, IL-17A-producing  $\gamma\delta$  T cells and ILC3 were evaluated by flow cytometric analysis in WT and *Tcr* $\delta^{-/-}$  mice after *S. aureus* colonization. Representative flow cytometric profiles of CD3 and lineage labeling on CD45<sup>+</sup>CD90<sup>+</sup>IL-17A<sup>+</sup> skin cells (left panels). The number of IL-17A<sup>+</sup>  $\gamma\delta$  T cells and ILC3

in WT and *Tcrδ*<sup>-/-</sup> mice (right panels). Results on right panels represent mean ± SD of 3 experiments. **H**, WT mice and *Tcrδ*<sup>-/-</sup> mice treated with control Ab and anti-CD90 Ab were epicutaneously colonized with *S. aureus*. Representative macroscopic images and HE-stained sections of mouse skin on day 7 after colonization (n=7 mice per group). Scale bars, 100 μm. **I–J**, Skin disease scores (**I**) and *S. aureus* CFU in the skin (**J**) of WT mice and *Tcrδ*<sup>-/-</sup> mice treated with control Ab and anti-CD90 Ab. Each dot represents a mouse. Results represent combined data of 2 independent experiments. ND; not detected, n.s.; not significant, \*P<0.05 and \*\*P<0.01, by using unpaired two-tailed Mann-Whitney U test (C–G) or by one-way ANOVA test with Bonferroni's correction (I, J).



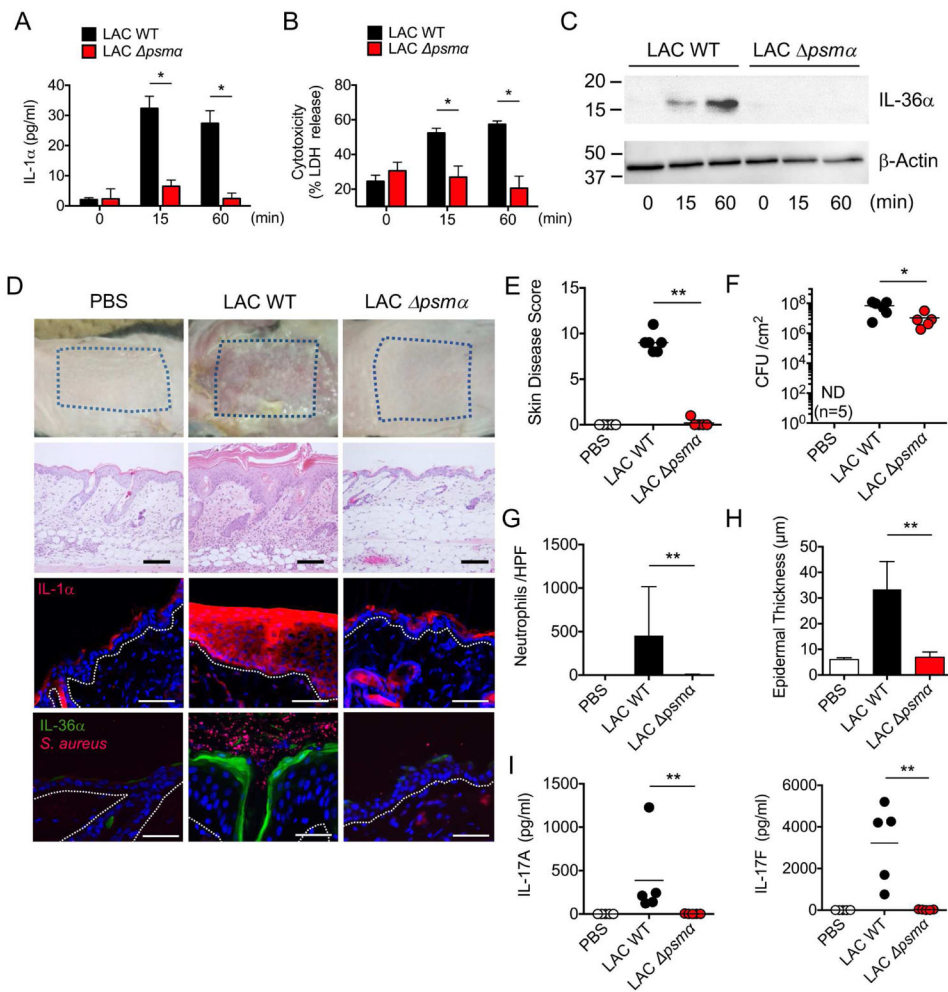


**Figure 6. PSM $\alpha$  peptides induce the release of keratinocyte IL-1 $\alpha$  and IL-36 $\alpha$  to mediate skin inflammation**

**A–B**, IL-1 $\alpha$  release (**A**) and cytotoxicity (**B**) of primary KCs from WT mice stimulated with culture supernatant of WT and *psma S. aureus* (LAC strain) for indicated time. Data are presented as mean  $\pm$  SD. **C**, IL-36 $\alpha$  release from primary KCs stimulated with culture supernatant of WT or *psma S. aureus* for indicated time. IL-36 $\alpha$  was detected by immunoblotting.  $\beta$ -actin in whole cell lysates is shown as loading control. **D**, Representative macroscopic images (top panels) and HE-stained sections (middle upper panels), and sections stained with Hoechst stain (blue) and antibody against IL-1 $\alpha$  (red) (middle lower panels) and stained with Hoechst stain (blue) and antibodies against *S. aureus* (red) and IL-36 $\alpha$  (green) (bottom panels) of the skin from WT mice colonized with WT and *psma S. aureus* or treated with PBS (n=5 to 8 per group) 7 days post infection. Epidermis/dermis border is marked by dotted white line. Scale bars, 100  $\mu$ m (middle upper panels), 50  $\mu$ m (middle lower panels) and 25  $\mu$ m (bottom panels). **E–H**, Day 7 skin disease scores (**E**), *S. aureus* CFU in the skin (**F**), quantification of neutrophils in the lesional skin (**G**) and epidermal thickening (**H**) of WT mice colonized with WT and *psma S. aureus* or treated with PBS (n=5 to 8 per group). Each dot represents a mouse (E, F, I). Data are presented as mean  $\pm$  SD (G, H). **I**, The amounts of IL-17A and IL-17F in the lesional skin of WT mice

colonized with WT or *psma S. aureus* or WT mice treated with PBS for 7 days. Each dot represents a mouse. Results represent combined data of 3 independent experiments. Data are representative of at least 2 independent experiments. ND; not detected, n.s.; not significant, \*P<0.05 and \*\*P<0.01, by unpaired, two-tailed Mann-Whitney U test.

Author Manuscript

Author Manuscript

Author Manuscript

Author Manuscript